

## Accepted Manuscript

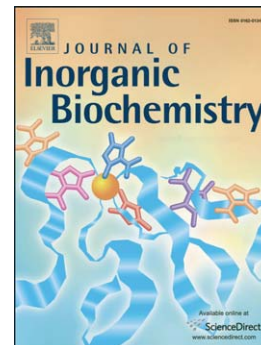
Metal coordination and tyrosinase inhibition studies with Kojic- $\beta$ Ala-Kojic

Joanna Izabela Lachowicz, Valeria Marina Nurchi, Guido Crisponi, Maria de Guadalupe Jaraquemada Pelaez, Antonio Rescigno, Piotr Stefanowicz, Marta Cal, Zbigniew Szewczuk

PII: S0162-0134(15)30028-3  
DOI: doi: [10.1016/j.jinorgbio.2015.07.001](https://doi.org/10.1016/j.jinorgbio.2015.07.001)  
Reference: JIB 9754

To appear in: *Journal of Inorganic Biochemistry*

Received date: 10 February 2015  
Revised date: 29 June 2015  
Accepted date: 1 July 2015



Please cite this article as: Joanna Izabela Lachowicz, Valeria Marina Nurchi, Guido Crisponi, Maria de Guadalupe Jaraquemada Pelaez, Antonio Rescigno, Piotr Stefanowicz, Marta Cal, Zbigniew Szewczuk, Metal coordination and tyrosinase inhibition studies with Kojic- $\beta$ Ala-Kojic, *Journal of Inorganic Biochemistry* (2015), doi: [10.1016/j.jinorgbio.2015.07.001](https://doi.org/10.1016/j.jinorgbio.2015.07.001)

This is a PDF file of an unedited manuscript that has been accepted for publication. As a service to our customers we are providing this early version of the manuscript. The manuscript will undergo copyediting, typesetting, and review of the resulting proof before it is published in its final form. Please note that during the production process errors may be discovered which could affect the content, and all legal disclaimers that apply to the journal pertain.

**Metal coordination and tyrosinase inhibition studies with Kojic- $\beta$ Ala-Kojic.**

Joanna Izabela Lachowicz\*<sup>a</sup>, Valeria Marina Nurchi<sup>a</sup>, Guido Crisponi<sup>a</sup>, Maria de Guadalupe Jaraquemada Pelaez<sup>a</sup>, Antonio Rescigno<sup>b</sup>, Piotr Stefanowicz<sup>c</sup>, Marta Cal<sup>c</sup> and Zbigniew Szewczuk<sup>c</sup>

<sup>a</sup> *Department of Chemical and Geological Sciences, University of Cagliari, Cittadella Universitaria, Monserrato, Cagliari, 09042, Italy*

<sup>b</sup> *Department of Biomedical Sciences, University of Cagliari, Cittadella Universitaria, Monserrato, Cagliari, 09042, Italy*

<sup>c</sup> *Faculty of Chemistry, University of Wrocław, F. Joliot-Curie 14, Wrocław, 50-383, Poland*

**Keywords:** Tyrosinase inhibitor, Kojic acid, Synthesis, Metal complexes

**Corresponding author:** J.I. Lachowicz; E-mail: lachowicz@unica.it; Phone +39 070 675 4471; Fax +39 070 675 4478; Department of Chemical and Geological Sciences, University of Cagliari, Cittadella Universitaria, Monserrato, Cagliari, Italy;

**Abstract**

Kojic acid is a natural antifungal and antibacterial agent that has been extensively studied for its tyrosinase inhibitory and metal coordination properties. Tyrosinase is a metalloenzyme with two copper ions in the active site. It is widely accepted that the tyrosinase inhibitory activity of kojic acid is related to its ability to coordinate metals. Over the past five years, we have used kojic acid to synthesize new and efficient bis-kojic acid chelators of iron and aluminium. In parallel, we investigated whether the de novo designed ligands could interfere with proper tyrosinase functioning. The present study combines our experience with inhibition and coordination studies of the new ligand: Kojic- $\beta$ Ala-Kojic. Research aimed at the assembly of a new potent tyrosinase inhibitor was based on the well-known crystal structure of the enzyme. Two questions were whether two kojic acids could act better than one and to what extent the length and kind of linker could ameliorate metal coordination, and inhibitory activity. Our results show that Kojic- $\beta$ Ala-Kojic has high affinity for Fe(III), Al(III), Zn(II), Cu(II) and strong tyrosinase inhibitory effect and it can be proposed for use in industrial and pharmaceutical applications.

## 1. Introduction

The compound 5-Hydroxy-2-hydroxy-methyl- $\gamma$ -pyrone was discovered in the latter part of the 19<sup>th</sup> century and since 1916 is known as Kojic acid (KA) [1]. It is produced as an antibiotic by *Aspergillus* and *Penicillium* species and inhibits the enzymatic activity of mushroom tyrosinase [2] (EC 1.14.18.1), an ubiquitous enzyme containing two copper ions. The dinuclear copper center of tyrosinase catalyzes the ortho-hydroxylation of monophenols, oxidation of catechols [3], quinonization of dihydroxycoumarins [4], o-aminophenols and aromatic o-diamines [5; 6].

The active site of tyrosinases exists in three states: deoxy-tyrosinase, oxy-tyrosinase and met-tyrosinase [7] (Scheme 1). The conversion of met- to deoxy-tyrosinase requires a two-electron reduction step. The deoxy-form can reversibly fix molecular oxygen leading to the oxy form. Although the mechanism of the reaction is not fully understood, it is generally accepted that ortho-diphenol oxidation occurs via Michaelis-Menten kinetics, whereas monophenols hydroxylation is characterized by a phase of latency [8]. Both cresolase and catecholase cycles produce ortho-quinones, which are further spontaneously rearranged into polymeric pigments [9].

### <Scheme 1>

The copper binding site is located at the heart of two pairs of hydrophilic antiparallel  $\alpha$ -helices [10]. Each of the two copper ions is coordinated by 3 histidine residues: Cu-A by His61, His85 and His94; Cu-B by His259, His263 and His296 [10]. The side chain rotational freedom is limited by histidine hydrogen bonds (61, 94, 259, 263) to peptide carbonyl oxygen atom as well as phenylalanine wedged between histidines (Phe90 between His94, His259, His296 and Phe292 between His61, His263, His296). Furthermore, His85, is covalently linked via a thioether to Cys83 which fixes the orientation

of the histidine side chain [10]. The exact role of this post-translationally formed thioether bond remains unclear but a direct role in catalysis can be excluded because it is not conserved [11].

Because the metal ion  $\text{Cu}^+$  is classified as a soft acid, it has a lower affinity for intermediate bases like imidazole and a higher affinity for interactions with thiol groups (soft bases). Bearing in mind that the Cys83-Met85 thioether bond is contained within the flexible loop connecting the rotating helices  $\alpha 3$  and  $\alpha 4$ , we hypothesized a structural role for cysteine residue in the deoxy form of tyrosinase.

The metal coordinating sphere is hydrophilic and located within the aromatic hydrophobic shell of phenylalanines. The Cu-B site is more rigid than the Cu-A site which contains histidine residues in different helices (His61 at the end of helix  $\alpha 3$ , His94 at the beginning of  $\alpha 4$ , His85 in the loop connecting  $\alpha 3$  and  $\alpha 4$ ).

Several previous reports have described kojic acid and its derivatives as inhibitors of melanin formation, both in vitro and in vivo [12; 13], speculating a possible role for copper coordination mechanisms [14]. In 2011, Fishman et. al. determined a tyrosinase structure from *Bacillus megaterium* (TyrBm) with bound kojic acid, the first tyrosinase structure with a bound ligand. The kojic acid molecule occupies identical positions in both subunits of TyrBm and is bound strongly by interactions with Phe, Pro, Asn and Arg residues. As opposed to the previously suggested modes for copper complex formation, the ligand was oriented with the hydroxymethyl towards the active site at the relatively far distance of 7 Å. Hence, the position and orientation of kojic acid causes an obstruction of the active site that could lead to inhibition of the tyrosinase enzyme.

In literature different kojic acid derivatives are reported as tyrosinase inhibitors. These studies mainly investigated the ability of the synthesized kojic acid derivatives to improve inhibitory properties by converting the methylene hydroxyl group into ester [15], hydroxylphenyl ester [16], glycoside [17] and amino acid derivatives [18-21].

Kojic acid was reported as well as chelating agent for trivalent and bivalent metal ions [22-25]. Encouraged by the promising results obtained in our previous reports of L1-L9 kojic acid derivatives (Figure 7, names of the ligands previously published as iron(III) and aluminium(III) chelators) [26-30], we focused the present study on the synthesis of Kojic- $\beta$ Ala-Kojic. We studied iron(III), aluminium(III), zinc(II) and copper(II) complexes and compared the results with previously published data. Moreover, we evaluated the tyrosinase inhibition efficacy of the new molecule and compared with low effective inhibitors of melanin [27-30] in order to know whether two kojic acids were better than one and if the length and kind of linker could improve inhibitory activity.

The ligand protonation and complex formation constants with copper were studied and compared with the results of low effective inhibitors.

## 2. Experimental

### 2.1 Reagents

HCl, KCl, KOH, D<sub>2</sub>O and ethanol were Sigma Aldrich products; 5-hydroxy-2-hydroxymethyl-pyran-4-one was obtained from TCI EUROPE N.V. Carbonate free potassium hydroxide solutions were prepared according to Albert and Serjant [31]. All chemicals used for synthesis (Tos-OSu, dioxane, triethylamine, ethyl acetate, DMSO and MgSO<sub>4</sub>) were purchased from Sigma Aldrich.

### 2.2 Synthesis of (5-hydroxy-4-oxo-4H-pyran-2-yl)methyl 3-((5-hydroxy-4-oxo-4H-pyran-2-yl)methoxy)carbonylamino)propanoate (Kojic- $\beta$ Ala-Kojic, K $\beta$ AK).

The synthesis was performed according to a recently described method [32] (Scheme 2).

#### <Scheme 2>

Kojic acid (5.4 g, 38 mmol) and Tos-OSu (5.6 g, 21 mmol) [33; 34] were suspended in 40 mL of dioxane followed by dropwise addition of triethylamine (8 mL). After stirring the reaction mixture at

65°C for 1 h, the solvent was evaporated under reduced pressure. After extracting the sample using a saturated sodium carbonate solution, the water fraction was acidified with HCl. The reaction product was extracted with ethyl acetate and dried over MgSO<sub>4</sub>. The solvent was then evaporated and further purified by preparative HPLC according to the procedure described in section 2.2.2. Sample identity and purity were confirmed by NMR (Figure S1), ESI-MS (Electrospray Ionization-Mass Spectrometry) (Figure S2) and HPLC.

Analytical data: 92% yield, ESI-MS Found: 382.0810 *m/z*; calculated 382.0769 *m/z* for (C<sub>16</sub>H<sub>15</sub>NO<sub>10</sub>)<sup>+</sup>, <sup>1</sup>H NMR (DMSO – d<sub>6</sub>, 500 MHz) δ 2.50 (t, 2H, J = 6.6Hz), 3.18 (q, 2H, J = 6.4Hz, J=12.72Hz), 4.78 (s, 1.8H), 4.87 (s, 2H), 6.30 (s, 1H), 6.39 (s, 1H), 7.50 (t, 0.8H, J = 5.5Hz), 7.99 (m, 2H). <sup>13</sup>C NMR (DMSO-d<sub>6</sub>, 500 MHz) δ 33.64, 36.41, 61.2, 61.3, 111.9, 112.5, 139.7, 139.8, 146.0, 155.1, 161.4, 162.5, 170.5, 173.6.

### 2.2.1 Synthesis of 1-[[4-Methylphenyl)sulfonyl]oxy]pyrrolidine-2,5-dione (Tos-OSu)

The protocol used for the synthesis of Tos-OSu was similar to that previously described in the literature [33; 34]. Briefly, N-Hydroxyimide (93 mmol) and tosyl chloride (100 mmol) were dissolved in tetrahydrofuran (100 mL) and triethylamine (14.7 mL) was then added over 20 min. After 40 min, the solvent was removed *in vacuo* and 100 mL of 5% hydrochloric acid was added. The product was filtered off, washed twice with water and crystallized from ethyl acetate to give Tos-OSu. Analytical data: 92% yield, ESI-MS Found: 292.02 *m/z*; calculated 292.03 *m/z* for (C<sub>11</sub>H<sub>11</sub>NO<sub>5</sub>S +Na)<sup>+</sup>, <sup>1</sup>H NMR (CDCl<sub>3</sub>, 500 MHz) δ 2.44 (s, 3H), 2.76 (s, 4H), 7.35 (d, 2H, J = 8.4 Hz), 7.87 (d, 2H, J = 8.4 Hz). <sup>13</sup>C NMR (CDCl<sub>3</sub>, 500 MHz) δ 21.8, 25.4, 129.6, 130.3, 131.3, 147.3, 168.7.

### 2.2.2. Purification of Kojic-βAla-Kojic

Preparative reversed-phase HPLC was performed on a Tosoh TSKgel ODS-120T column (21.5 mm × 300 mm) (Tosoh, Tokyo, Japan) using the same solvent system, gradient 0.5% min<sup>-1</sup> and a flow rate of 7 mL min<sup>-1</sup>. The crude product was analyzed by analytical HPLC using a Thermo separation HPLC system with UV detection (210 nm) on a Vydac Protein RP C18 column (250×4.6 mm, 5 mm) (Grace, Deerfield, IL, USA), with a gradient elution of 0-80% B in A (A = 0.1% TFA in water; B = 0.1% TFA in acetonitrile - H<sub>2</sub>O, 4 : 1) for 45 min (flow rate 1 mL mL<sup>-1</sup>, rt).

### 2.3. *Spectrophotometric–potentiometric measurements*

The combined spectrophotometric-potentiometric method used in the present study has been previously described [26]. Ligand concentration (depending on absorptivity values) was 0.5mM. Spectra were recorded in the 200–400 nm spectral range using a 0.2 cm path length. Iron(III) complex formation studies were made with the use of 0.5mM ligand concentration and metal to ligand molar ratio 1:1. The Vis spectra were recorded in the 300-800 nm range using a 1 cm path length. The Al(III), Cu(II) and Zn(II) complexes were studied with the use of only potentiometric method; 0.5mM ligand concentration and metal to ligand molar ratio 1:1. Potentiometric data were processed using Hyperquad2013 software [35], while spectrophotometric data were obtained by the HypSpec program [36].

### 2.4. *NMR measurements*

<sup>1</sup>H NMR spectra were collected on a Bruker Advance 300 spectrometer at 300.13 MHz in DMSO with a 5 mm sample tube at 25<sup>0</sup>C; chemical shifts were referenced to residual solvent signal (3.5 ppm).

### 2.5. *ESI–MS analysis of complexes*

All MS experiments were performed on a Bruker microTOF-Q spectrometer (BrukerDaltonik, Bremen, Germany), equipped with an Apollo II electrospray ionization source with an ion funnel. The instrument parameters have been previously described [30]. Collision energy was optimized for each product to obtain the best fragmentation. The solutions of 0.1mM ligand with 0.1mM metal ions were prepared in water:methanol (50:50) and incubated for 24h before measurements.

## 2.6. Enzyme Extraction, purification and tyrosinase activity

The mushroom tyrosinase (EC 1.14.18.1) from *Agaricus bisporus* was purified as previously described [37]. Tyrosinase inhibitory activity was determined by a spectrophotometric method. The compound solution was prepared in 10% DMSO solution. Each sample was diluted in a test tube with 0.05 M sodium phosphate buffer (pH 6.8). This was followed by the addition of 0.04-0.35 mL (S)-2-Amino-3-(3,4-dihydroxyphenyl)propanoic acid (L-DOPA, 10 mM) solution (in 10 mM acetic acid) and 0.034 mL mushroom tyrosinase (200 units/mL). The 2.000 mL solution was mixed, incubated for 10 min at 25<sup>0</sup>C and the absorbance measured at 476 nm. The experiment was repeated with different inhibitor concentrations: 0.069, 0.139 and 0.279 mM. The absorbance of the same mixture without inhibitor was used as control with the addition of 10% DMSO water solution for its inhibitory effect. The percent inhibition of tyrosinase activity was calculated using the equation below:

$$\% \text{ inhibition} = (A-B)/A \times 100$$

where A represents the absorbance at 476 nm without the test sample, and B represents the absorbance at 476 nm with the test sample at the same substrate concentration.

In order to calculate IC<sub>50</sub> values, 2 mM stock solutions of tyrosinase inhibitors (kojic acid and KβAK) were prepared in 10% ethanol/water mixture. IC<sub>50</sub> values were determined after addition of various inhibitors amounts to enzyme assays to determine a range of inhibitors needed to encompass the IC<sub>50</sub> value. Each 1 mL assay contained a fixed amount of enzyme, inhibitor, 3 mM L-DOPA (final concentration), and 100 mM phosphate buffer (final concentration) pH 6.5. The inhibition was also

characterized in terms of an  $IC_{50}$  value by using GraFit Version 7.0.3 program (Erithacus Software Ltd., Horley, Surrey, UK) based on the following equation:

$$y = \frac{Range}{1 + \left(\frac{x}{IC_{50}}\right)^s} + Background$$

where *Range* is the maximum y range, and *s* is a slope factor. The *x* axis represents the concentration of analyte. Data fitted to this equation are displayed with a logarithmically scaled *x* axis.

### 3. Results and discussion

#### 3.1. Ligand deprotonation

The new ligand K $\beta$ AK has three potential protonation sites and indeed we determined three protonation constants from combined potentiometric-UV titration data calculated by HypSpec software [36] (Table 1). In Figure 1, the four molar absorptivity spectra are reported, each representing a differently protonated form. The [LH<sub>3</sub>]<sup>+</sup> band has the highest intensity at 268 nm ( $\epsilon=10998 \text{ M}^{-1}\text{cm}^{-1}$ ). The first deprotonation at pH 2.9 can be attributed to nitrogen atom and does not significantly change the spectrum. The [LH<sub>2</sub>] band displays maximum intensity at 268 nm and does not differ in shape from the band of the fully protonated ligand. The two kojic acid units are separated by the hydrophobic linker and ligand is not symmetric; each kojic unit deprotonates at different pH levels: 7.15 and 8.44. The [LH]<sup>-</sup> and [L]<sup>2-</sup> bands are different: [LH]<sup>-</sup> band presents two maxima at 250 nm ( $\epsilon=6400 \text{ M}^{-1}\text{cm}^{-1}$ ) and 317 nm ( $\epsilon=5403 \text{ M}^{-1}\text{cm}^{-1}$ ); the [L]<sup>2-</sup> band has a maximum absorptivity at 317 nm ( $\epsilon=8218 \text{ M}^{-1}\text{cm}^{-1}$ ). The charge of the molecule depends on the pH of the solution (Figure 2); negatively charged forms are in equilibrium at neutral pH.

<Figure 1>

<Figure 2>

## &lt;Table 1&gt;

The first and second protonations attributed to the kojic acid units differ significantly from the kojic acid protonation constant (7.70 [26]). This is due to the formation of the intramolecular hydrogen bonds previously reported by us for kojic acid derivatives [26-28; 30].

3.2. *Complex formation studies*3.2.1. *Copper and zinc complexes*

K $\beta$ AK forms mononuclear complexes with copper ions at pH 2, which become dinuclear complexes at pH 3. The presence of one proton in the [CuLH]<sup>+</sup> complex can be attributed to one kojic acid unit, and discards the possibility of ring-closed mononuclear coordination. At pH 6.23, the [Cu<sub>2</sub>L<sub>2</sub>] complex is formed, while at pH 7.28, 8.83 we observe displacement of protons of the water molecules in the coordination sphere (Figure 4). The ESI-MS studies of the copper complexes at neutral pH (Figure S4, S5) confirm the formation of [CuLH]<sup>+</sup> and [Cu<sub>2</sub>L<sub>2</sub>H]<sup>+</sup> complexes.

The interesting results arising from the ms/ms experiment (Figure S7) with mononuclear complex (442.994 m/z) make it possible to locate the metal ion in the unsymmetrical complex. Figure 3 shows the possible fragments that can be obtained from the two different complexes reported as A and Z, respectively. In Table 2 and Figure 3, with the exception of the A5-Z5 and A6-Z6 pairs, we can see that A1 fragment of the complex is equal to Z1, A2 to Z2 and so forth. A6, Z6 and A5 fragments are not present in the spectrum, while Z5 yields an intensive signal. The presence of Z5 suggests that metal coordination by kojic acid (B) occurs closer to the nitrogen atom. The simulated spectra are in perfect agreement with the observed signals (Figure S6-8, Table S1).

## &lt;Table 2&gt;

## &lt;Figure 3&gt;

## &lt;Figure 4&gt;

The stoichiometry of the zinc complexes is not different from that of copper complexes (Figure 4), although the zinc complexes are weaker (Table 3). The pZn (6.1) value is much lower than pCu (8.3).  $[\text{ZnLH}]^+$  complexes start to form at pH 4, whereas  $[\text{Zn}_2\text{L}_2\text{H}]^+$  complexes start to form at pH 5. At pH 7.9, the  $[\text{Zn}_2\text{L}_2]$  complex is formed and at pH 9.44 water molecules in the coordination sphere are deprotonated. The mono- and dinuclear complexes were confirmed by the ESI-MS experiments (Figure S10). The ms/ms experiment (Figure S11) with  $[\text{ZnLH}]^+$  complex (443.99  $m/z$ ) shows the coordination of zinc ions by the B kojic acid unit (Table S2, Figures S12,S13).

### 3.2.2. Iron and aluminium complexes

The ligand starts forming monomeric complexes with iron ions at pH lower than 1. Their presence is indicated by the spectra within the range of 400-700 nm (Figure 5). The values for molar absorptivity with maximum absorption at 500 nm correspond to those of kojic acid complexes, confirming the formation of mononuclear complex. At pH 2, dinuclear complexes form with water molecules in the coordination sphere. In ESI-MS spectrum (Figure S9) we can observe an intensive signal at 434.995  $m/z$  corresponding to  $[\text{Fe}_2\text{L}_2]^{2+}$  complex (Figure S9, Panel A) and a low intensity signal at 453.005  $m/z$  corresponding to  $[\text{FeL}(\text{H}_2\text{O})]^+$  complex (Figure S9, Panel B). The signal indicating  $[\text{FeL}(\text{H}_2\text{O})]^+$  could refer to a breakdown product of the  $[\text{Fe}_2\text{L}_2(\text{H}_2\text{O})_2]^{2+}$  complex (Figure S9 Panel D) that we observe deprotonated at neutral pH.

<Figure 5>

<Figure 6>

The stoichiometry of aluminium complexes is the same as that of iron complexes, although the pAl value (12.7) is lower than the pFe value (18.5) (Table 3). The mononuclear complex  $[\text{AlLH}]^+$  exists from pH 2 to pH 6 (Figure 6). The dinuclear complex  $[\text{Al}_2\text{L}_2\text{H}]$  starts to form at pH 3 and at pH 4.3 loses its last proton. The presence of mono (single charged) and dinuclear (double charged) complexes is confirmed by two overlapping signals at 406.039  $m/z$  in the ESI-MS spectrum (Figure S3 and Figure

S3.1.). Two of the coordination water molecules in the coordination sphere are forming most likely bridges between two aluminium ions. In the ESI-MS spectrum (Figure S3) we observe a signal at 424.050  $m/z$  for  $[AlL(H_2O)]^+$ , which confirms the importance of water in the complex structure. The signal corresponding to  $[AlL(H_2O)]^+$  could indicate a breakdown product of the  $[Al_2L_2(H_2O)_2]^{2+}$  complex that we observe deprotonated at neutral pH.

<Table 3>

### 3.3. Tyrosinase inhibition studies

Over the past 5 years we have synthesized several different kojic acid derivatives (Figure 7) with the aim of individuating effective iron and aluminium chelating agents. One of the requisites of a ligand used in chelation therapy is that it must not interfere with proper enzymatic activity. This issue was carefully considered when evaluating our molecules for tyrosinase inhibitory activity. In the present study, we compare the results obtained on the tyrosinase inhibitory activity of seven biskojic derivatives and a mono kojic derivative L7.

<Figure 7>

<Figure 8>

In Figure 8, the percentage inhibition of kojic acid (84%) is compared with that of its analogues. The results show that K $\beta$ AK has the highest inhibition efficiency (91%), ligands L1-L5 have low inhibition efficiency (24-36%), while L6 and L7 have no influence whatsoever on tyrosinase activity.

Based on these preliminary results, we decided to investigate the inhibitory activity of the most promising ligand K $\beta$ AK and compare with KA. Figure 9 shows the activity of the enzymes (Ctrl 1 and Ctrl 2) acting on the substrate L-tyrosine after 30 (A) and 90 min (B), respectively. At increasing concentrations of KA, the tyrosinase-mediated formation of the pigment dopachrome was delayed after 30 min (Figure 9A). In the presence of K $\beta$ AK at the same concentration, the inhibitory activity became

much stronger, as demonstrated by the complete lack of melanin formation even after 90 min of incubation (Figure 9B).

IC<sub>50</sub> values for tyrosinase inhibitors can vary for a number of reasons, including choice of assay conditions, rate determinations, solvent considerations, and also the purity of the tyrosinase [38]. For instance, reported IC<sub>50</sub> values for kojic acid vary from 10 to 300 μM [38]. Under our experimental conditions the IC<sub>50</sub> value for KβAK was equal to 6.8±0.9 μM, whereas that of kojic acid was amounting to 35.4±4.3 μM. Although our findings cannot explain the mechanism of KβAK inhibition, we can notice that the IC<sub>50</sub> of the new inhibitor is approximately 1/5 that of kojic acid. This result is lower than that of most effective Kojic-Phenylalanine-Kojic (1/382) reported in the literature [15].

<Figure 9>

Our tyrosinase inhibition studies were performed and compared with the data of Kobayashi et al. prepared under the same experimental conditions [15]. Nevertheless, the extracted mushroom enzymes had low homology with the more complex mammalian ones (22-24% sequence identity with 48-49% sequence coverage) [39]. Recent [39] reports suggest that inhibition studies with human tyrosinase could be more informative.

The two-step synthesis of KβAK is time and cost-saving in comparison with the multi-step synthesis of other kojic acid derivatives as tyrosinase inhibitors [15; 21]. In the catalytic activity test, KβAK proved to be a better inhibitor than kojic acid, and above all, was far more effective after 30 and 60 min (Figure 9). This strong inhibitory effect cannot be explained by the contemporary presence of two kojic acid units, since the L1-L6 and L9 ligands possess two kojic acid units and are less effective than KβAK and even kojic acid alone. Neither is L7 an antagonist of tyrosinase activity. Initially, we hypothesized that the presence of an aromatic ring in the ligand structure (L2, L3, L5, and L7) could facilitate docking into the active site of tyrosinase, similarly to kojic acid conjugates with phenylalanine

[15]. According to this hypothesis, Phe90 residue could form  $\pi$ - $\pi$  stacking interactions between the aromatic rings of the linker. However, the results of our laboratory tests showed exactly the contrary. Neither the hydrophilic chain between the two kojic units of L9, nor the shorter and more hydrophobic chains of L1 and L4 resulted to be capable of increasing inhibitory activity, the latter two yielding slightly better results.

#### 4. Conclusions

The neutral form of K $\beta$ AK at physiological pH together with its low molecular weight suggests high bioavailability. The chemical properties are in agreement with Lipinski's rules [40] for orally active drug (no more than 5 hydrogen bonds; no more than 10 hydrogen bond acceptors; a molecular mass less than 500 Daltons) and candidate it for pharmaceutical applications.

K $\beta$ AK form with Fe(III), Al(III), Cu(II) and Zn(II) metals mono- and dinuclear complexes. The molecule is selective for trivalent ions with pFe and pAl higher than pCu and pZn values. The strength of iron and aluminium complexes with K $\beta$ AK is similar to those formed with L2 and L4 (Table 4). Among previously synthesized bis-kojic acid derivatives, K $\beta$ AK is the weakest copper and zinc chelator.

#### <Table 4> [26-30; 41; 42]

L1-L6 and L9 ligands form [CuL] and [Cu<sub>2</sub>L<sub>2</sub>] complexes, while KA and L7 ligands form [CuL<sub>2</sub>] complexes. The strength of the complexes, evaluated by pCu values (the higher the pCu the stronger the coordination), does not influence the inhibitory properties. In fact, the most effective inhibitory ligands (kojic acid and K $\beta$ AK) had the lowest pCu values (Table 4).

The mechanisms underlying kojic acid inhibition are not yet fully understood and although our findings offer some insight, further research is warranted to explore this topic.

In conclusion, the key to success of the K $\beta$ AK as a tyrosinase inhibitor could rely on the peculiarities of the chain between the two kojic acid units. Indeed, its hydrophobic properties are sufficient to allow for a perfect fit into the active site of the enzyme, without creating any unconformity with Phe90. However, this hypothesis is based solely on results obtained in the laboratory and needs to be confirmed by computational studies of docking and crystallographic data.

### Acknowledgments

GC and JIL acknowledge RAS for financial support CRP-27564 and VMN for CRP-26712.

### References

- [1] R. Kinosita, T. Shikata, *Mycotoxins in Foodstuffs*. MIT Press. Cambridge, Massachusetts (1964).
- [2] R. Saruno, F. Kato, T. Ikeno, *Agric. Biol. Chem.* 43 (1979) 1337-1338.
- [3] P. Zucca, E. Sanjust, M. Loi, F. Sollai, M. Ballero, M. Pintus, A. Rescigno, *Phytochemistry*, 90 (2013) 16-24.
- [4] F. Sollai, P. Zucca, E. Sanjust, D. Steri, A. Rescigno, *Biol. Pharm. Bull.* 31 (2008) 2187-2193.
- [5] F. Bruyneel, O. Payen, A. Rescigno, B. Tinant, J. Marchand-Brynaert, *Chem. Eur. J.* 15 (2009) 1521-3765.
- [6] A. Rescigno, F. Bruyneel, A. Padiglia, F. Sollai, A. Salis, J. Marchand-Brynaert, E. Sanjust, *Biochim. Biophys. Acta* 1810 (2011) 799–807.
- [7] S. Halaouli, M. Asther, J.C. Sigoillot, M. Hamdi, A. Lomascolo, *J. App. Microbiol.* 100 (2006) 219-232.
- [8] Á. Sánchez-Ferrer, J. Neptuno Rodríguez-López, F. García-Cánovas, F. García-Carmona, *Biochim. Biophys. Acta* 1247 (1995) 1-11.
- [9] J.N. Rodriguez-Lopez, J. Tudela, R. Varon, F.J. Garcia-Carmonas, *J. Biol. Chem.* 267 (1992) 3801–3810.
- [10] W.T. Ismaya, H. Rozeboom, A. Weijn, J. Mes, F. Fusetti, H. Wichers, B.W. Dijkstra, *Biochemistry* 50 (2011) 1520-4995.
- [11] T. Klabunde, C. Eicken, J.C. Sacchettini, B. Krebs, *Nat. Struct. Biol.* 12 (1998) 1084–1090.
- [12] V. Kahn, N. Ben-Shalom, V. Zakin, *J. Agricul. Food Chem.* 45 (1997) 4460-4465.

- [13] Y. Mishima, S. Hatta, Y. Ohyama, M. Inazu, *Pigm. Cell. Res.* 1 (1988) 367-374.
- [14] M. Sendovski, M. Kanteev, V.S. Ben-Yosef, N. Adir, A. Fishman, *J. Mol. Biol.* 405 (2011) 227-237.
- [15] Y. Kobayashi, H. Kayahara, K. Tadasa, H. Tanaka, *Bioorg. Med. Chem. Lett.* 6 (1996) 1303-1308.
- [16] J. Kadokawa, T. Nishikura, R. Muraoka, H. Tagaya, N. Fukuoka, *Synth. Comm.* 33 (2003) 1081-1086.
- [17] T. Nishimura, T. Kometani, H. Takii, Y. Terada, S. Okada, *J. Ferm. Bioeng.* 78 (1994) 37-41.
- [18] G. O'Brien, J. Patterson, J. Meadow, *J. Org. Chem.* 27 (1962) 1711-1714.
- [19] Y. Kobayashi, H. Kayahara, K. Tadasa, T. Nakamura, H. Tanaka, *Biosci. Biotech. Biochem.* 59 (1995) 1745-1746.
- [20] H. Kim, J. Choi, J.K. Cho, S.Y. Kim, Y.-S. Lee, *Bioorg. Med. Chem. Lett.* 14 (2004) 2843-2846.
- [21] J.M. Noh, S.Y. Kwak, D.H. Kim, Y.S. Lee, *Pep. Scien.* 88 (2007) 300-307.
- [22] B.E. Bryant, C. Fernelius, *J. Am. Chem. Soc.* 76 (1954) 5351-5352.
- [23] W. McBryde, G. Atkinson, *Can. J. Chem.* 39 (1961) 510-525.
- [24] T. Hedlund, L.O. Öhman, *Acta Chem. Scan. A* 42 (1988) 702-709.
- [25] M.M. Finnegan, T.G. Lutz, W.O. Nelson, A. Smith, C. Orvig, *Inorg. Chem.* 26 (1987) 2171-2176.
- [26] V.M. Nurchi, G. Crisponi, J.I. Lachowicz, S. Murgia, T. Pivetta, M. Remelli, A. Rescigno, J. Niclós-Gutierrez, J.M. González-Pérez, A. Domínguez-Martín, *J. Inorg. Biochem.* 104 (2010) 560-569.
- [27] V.M. Nurchi, J.I. Lachowicz, G. Crisponi, S. Murgia, M. Arca, A. Pintus, P. Gans, J. Niclos-Gutierrez, A. Diminguez-Martin, A. Castineiras, M. Remelli, Z. Szewczuk, T. Lis, *Dalton Trans.* 40 (2011) 5984-5998.
- [28] L. Toso, G. Crisponi, V.M. Nurchi, M. Crespo-Alonso, J.I. Lachowicz, M. A. Santos, S. M. Marques, J. Niclos-Gutierrez, J.M. Gonzalez-Perez, A. Diminguez-Martin, D. Choquesillos-Lazarte, Z. Szewczuk, *J. Inorg. Biochem.* 127 (2013) 220-231.
- [29] L. Toso, G. Crisponi, V.M. Nurchi, M. Crespo-Alonso, J.I. Lachowicz, D. Mansoori, M. Arca, M. A. Santos, S. M. Marques, L. Gano, J. Niclos-Gutierrez, J.M. Gonzalez-Perez, A. Diminguez-Martin, D. Choquesillos-Lazarte, Z. Szewczuk, *J. Inorg. Biochem.* 130 (2014) 112-121.
- [30] V.M. Nurchi, G. Crisponi, M. Arca, M. Crespo-Alonso, J.I. Lachowicz, D. Mansoori, L. Toso, G. Pichiri, M. A. Santos, S. M. Marques, J. Niclos-Gutierrez, J.M. Gonzalez-Perez, A. Diminguez-

- Martin, D. Choquesillos-Lazarte, Z. Szewczuk, M.A. Zoroddu, M. Peana, J. Inorg. Biochem. 141 (2014) 132-143.
- [31] A. Albert, E. Serjeant, The determination of ionization constants, Chapman and Hall, London, New York, 1984.
- [32] M. Cal, M. Jaremko, Ł. Jaremko, P. Stefanowicz, Amino acids 44 (2013) 1085-1091.
- [33] P. Stefanowicz, Ł. Jaremko, M. Jaremko, T. Lis, New J. Chem. 30 (2006) 258-265.
- [34] C. Sheikh, S. Takagi, A. Ogasawara, M. Ohira, R. Miyatake, H. Abe, T. Yoshimura, H. Morita, Tetrahedron 66 (2010) 2132-2140.
- [35] <http://www.hyperquad.co.uk/HQ2013.htm>, (07-05-2015).
- [36] P. Gans, A. Sabatini, A. Vacca, Talanta 43 (1996) 1739-1753.
- [37] B. Marongiu, A. Piras, S. Porcedda, E. Tuveri, E. Sanjust, M. Meli, F. Sollai, P. Zucca, A. Rescigno, J. Agri. Food Chem. 55 (2007) 10022-10027.
- [38] E. Neeley, G. Fritch, A. Fuller, J. Wolfe, J. Wright, W. Flurkey, Intern. J. Mol. Scien. 10 (2009) 3811-3823.
- [39] S. Fogal, M. Carotti, L. Giaretta, F. Lanciani, L. Nogara, L. Bubacco, E. Bergantino, Mol. Biotech. (2015) 1-13.
- [40] C.A. Lipinski, F. Lombardo, B.W. Dominy, P.J. Feeney, Adv. Drug Del. Rev. 64 (2012) 4-17.
- [41] Joanna Izabela Lachowicz, et al., J. Inorg. Biochem. submitted (2015).
- [42] A. Okac, Z. Kolarik, Collect. Czech. Chem. Commun 24 (1959) 266-272.

## Figure Captions

**Scheme 1.** Schematic representation of the reactions at the catalytic center of fungal tyrosinase.

**Scheme 2.** Schematic representation of the synthesis of (5-hydroxy-4-oxo-4H-pyran-2-yl)methyl 3-({[(5-hydroxy-4-oxo-4H-pyran-2 yl)methoxy]carbonyl}amino)propanoate (Kojic-βAla-Kojic, KβAK).

**Figure 1.** Molar absorptivity spectrum of the new K $\beta$ AK ligand using the HypSpec program, 0.2 cm path length and ligand concentration  $5 \cdot 10^{-4}$  M. The charges have been omitted for simplicity.

**Figure 2.** Distribution diagram of the ligand calculated with the Log  $\beta$  values shown in Table 1, using  $5 \cdot 10^{-4}$  M ligand concentration.

**Figure 3.** Theoretical ms/ms fragments of the CuLH complex (442.997 m/z).

**Figure 4.** Speciation plots of ligand complexes with copper(II) (top) and zinc(II) (bottom) calculated on the basis of stability constants reported in Table 3 using a ligand concentration  $5 \cdot 10^{-4}$  M and metal to ligand molar ratio 1:1. Charges are omitted for simplicity.

**Figure 5.** Spectra of the [FeLH]<sup>2+</sup> complex in a pH range of 0.80-2.10 obtained using a ligand concentration  $5 \cdot 10^{-4}$  M and metal to ligand molar ratio 1:1 and 1 cm path length.

**Figure 6.** Speciation plots of ligand complexes with iron(III) (top) and aluminium(III) (bottom) calculated on the basis of stability constants reported in Table 3 using a ligand concentration  $5 \cdot 10^{-4}$  M and metal to ligand molar ratio 1:1. Charges are omitted for simplicity.

**Figure 7.** Molecular structures of previously studied tyrosinase inhibitors.

**Figure 8.** Diagram of tyrosinase inhibition. The percent inhibition of tyrosinase activity calculated as: % inhibition =  $(A-B)/A \times 100$ ; A represents the absorbance at 476 nm without the test sample, and B represents the absorbance at 476 nm with the test sample at the same substrate concentration. The experiment was repeated with different inhibitor concentrations: 0.069, 0.139 and 0.279 mM.

**Figure 9.** Inhibitory effect of KA and K $\beta$ AK on catalytic activity of mushroom tyrosinase after 30 min (A) and 90 min (B) of incubation. Two different concentrations (40 and 80  $\mu$ M) were tested.

**Table 1.** Protonation constants of the new ligand K $\beta$ AK calculated with HyperQuad2013 program at 25°C and 0.1 M KCl ionic strength using the ligand concentration  $5 \cdot 10^{-4}$  M . Charges are omitted for simplicity.

Specie	Log $\beta$	Log K
LH	8.44(4) <sup>a</sup>	8.44(4)
LH <sub>2</sub>	15.59(4) <sup>a</sup>	7.15(4)
LH <sub>3</sub>	18.5(1) <sup>a</sup>	2.9(1)

<sup>a</sup>Standard deviation values were calculated by the HyperQuad2013 program.

**Table 2.** Signals ( $m/z$  values) obtained for the fragments of the  $[\text{CuLH}]^+$  complex, using a ligand concentration  $1 \times 10^{-4} \text{ M}$  and metal to ligand molar ratio 1:1 in  $\text{H}_2\text{O}:\text{CH}_3\text{OH}$  (50:50) solution, pH 7.

Type	$m/z$	Type	$m/z$
A1	172.93*	Z1	172.93*
A2	186.94	Z2	186.94
A3	202.94	Z3	202.94
A4	230.93	Z4	230.93
A5	244.95*	Z5	245.95
A6	258.97*	Z6	259.96*
A7	273.98	Z7	273.98
A8	301.97	Z8	301.97
A9	317.97	Z9	317.97
A10	331.98*	Z10	331.98*

\* Fragments not present in the spectrum.

**Table 3.** Stability constants of metal complexes calculated with HyperQuad program at 25°C and 0.1 M KCl ionic strength using the ligand concentration  $5 \cdot 10^{-4}$  M and metal to ligand molar ratio 1:1. Charges are omitted for simplicity. Protonation constants of the ligands and overall stability constants ( $\log \beta_{pqr}$ ) of the metal complexes were calculated by using eqs:  $pM + qH + rL = M_pH_qL_r$ ,  $\beta_{pqr} = ([M_pH_qL_r]) / ([M]^p[H]^q[L]^r)$ .

Model	Fe <sup>3+</sup>	Al <sup>3+</sup>	Cu <sup>2+</sup>	Zn <sup>2+</sup>
MLH	18.7(1) <sup>a</sup>	15.75(2) <sup>a</sup>	15.03(7) <sup>a</sup>	13.07(5) <sup>a</sup>
M <sub>2</sub> L <sub>2</sub> H	-	30.32(8) <sup>a</sup>	29.23(4) <sup>a</sup>	24.45(2) <sup>a</sup>
M <sub>2</sub> L <sub>2</sub>	35.3(1) <sup>a</sup>	26.09(3) <sup>a</sup>	23.00(4) <sup>a</sup>	16.55(3) <sup>a</sup>
M <sub>2</sub> L <sub>2</sub> H <sub>-1</sub>	32.12(9) <sup>a</sup>	20.4(2) <sup>a</sup>	15.72(4) <sup>a</sup>	7.11(4) <sup>a</sup>
M <sub>2</sub> L <sub>2</sub> H <sub>-2</sub>	28.06(5) <sup>a</sup>	16.01(2) <sup>a</sup>	6.89(4) <sup>a</sup>	-
M <sub>2</sub> L <sub>2</sub> H <sub>-3</sub>	21.00(4) <sup>a</sup>	8.87(3) <sup>a</sup>	-	-
M <sub>2</sub> L <sub>2</sub> H <sub>-4</sub>	12.35(4) <sup>a</sup>	0.73(3) <sup>a</sup>	-12.63(6) <sup>a</sup>	-
M <sub>2</sub> L <sub>2</sub> H <sub>-6</sub>	-7.51(5) <sup>a</sup>	-18.3(2) <sup>a</sup>		
<b>pM*</b>	<b>18.5</b>	<b>12.7</b>	<b>8.3</b>	<b>6.1</b>

H<sub>n</sub> are referred to hydroxo complexes.

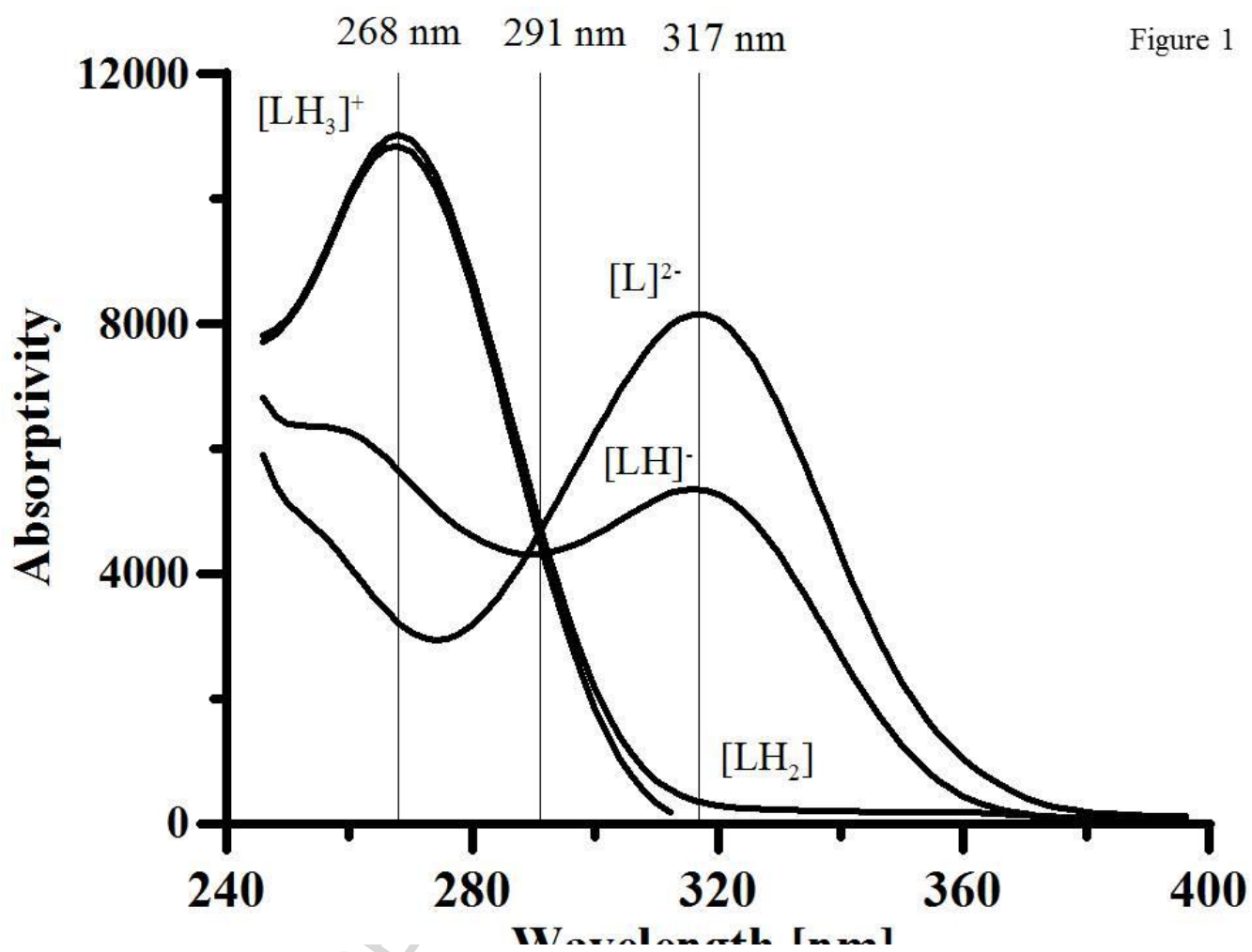
<sup>a</sup> Standard deviation values were calculated by the HyperQuad2013 program.

\* Negative logarithm of the concentration of the free metal in solution, calculated for total [ligand] =  $10^{-5}$  M and total [metal] =  $10^{-6}$  M at pH 7.4.

**Table 4.** Comparison of pM values for KA, L1-L9 and K $\beta$ AK ligands.

pM*	KA	L1	L2	L3	L4	L5	L6	L7	L9	K $\beta$ AK
<b>pFe</b>	13.3[26]	23.1[26]	18.9[27]	22.2[27]	18.1[28]	19.3[28]	17.7[28]	16.7[28]	17.7[30]	18.5
<b>pAl</b>	9.1[26]	12.8[26]	11.9[27]	13.9[27]	11.2[29]	11.6[29]	11.8[29]	9.9[29]	10.3[30]	12.7
<b>pCu</b>	7.3[44]	8.8[43]	10.2[43]	10.5[43]	10.3[43]	10.8[43]	8.5[43]	7.2[43]	9.7[30]	8.3
<b>pZn</b>	6.1[44]	6.6[43]	7.6[43]	7.9[43]	8.8[43]	7.1[43]	7.8[43]	6.1[43]	7.6[30]	6.1

\* Negative logarithm of the concentration of the free metal in solution, calculated for total [ligand] =  $10^{-5}$ M and total [metal] =  $10^{-6}$ M at pH 7.4.



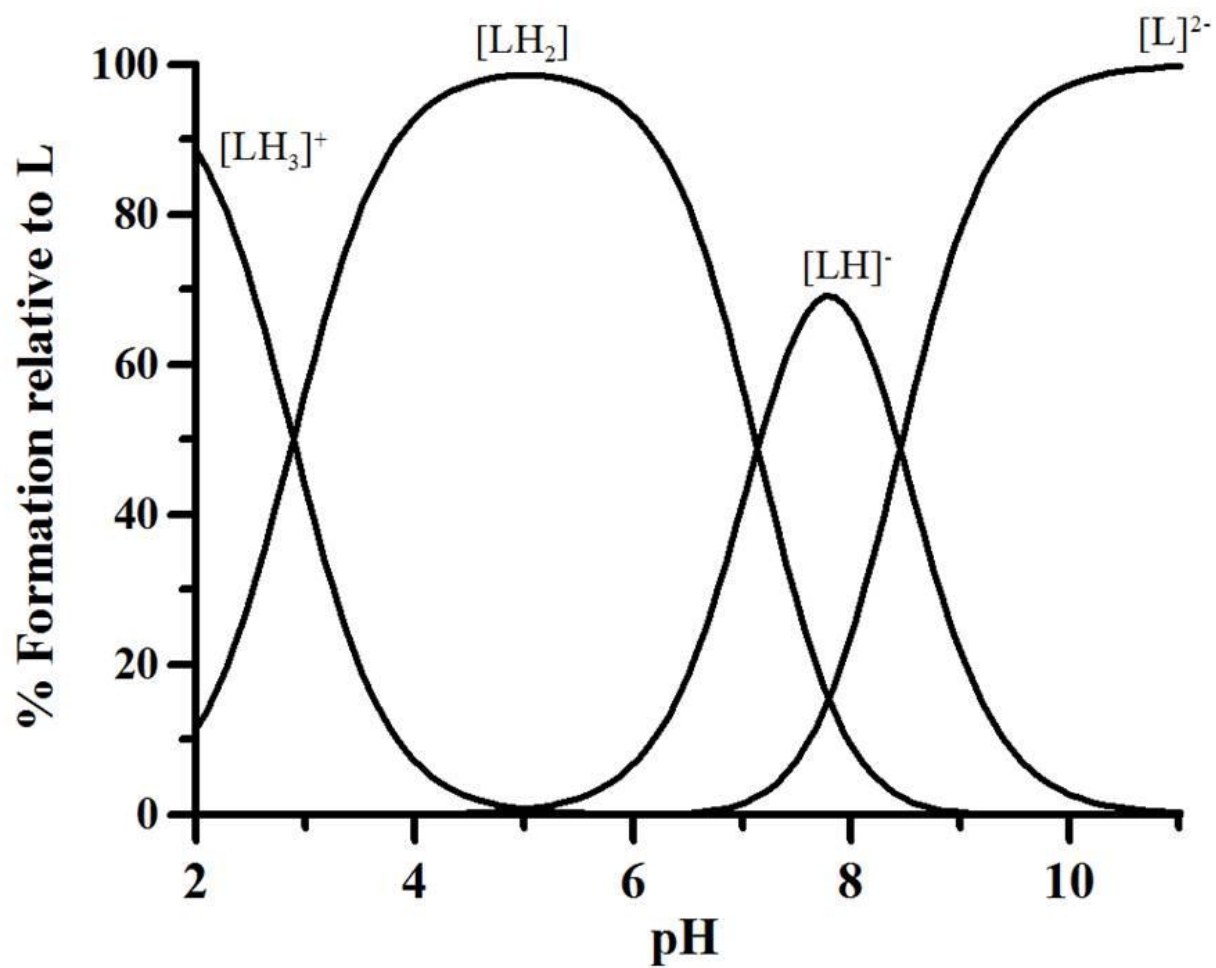


Figure 2

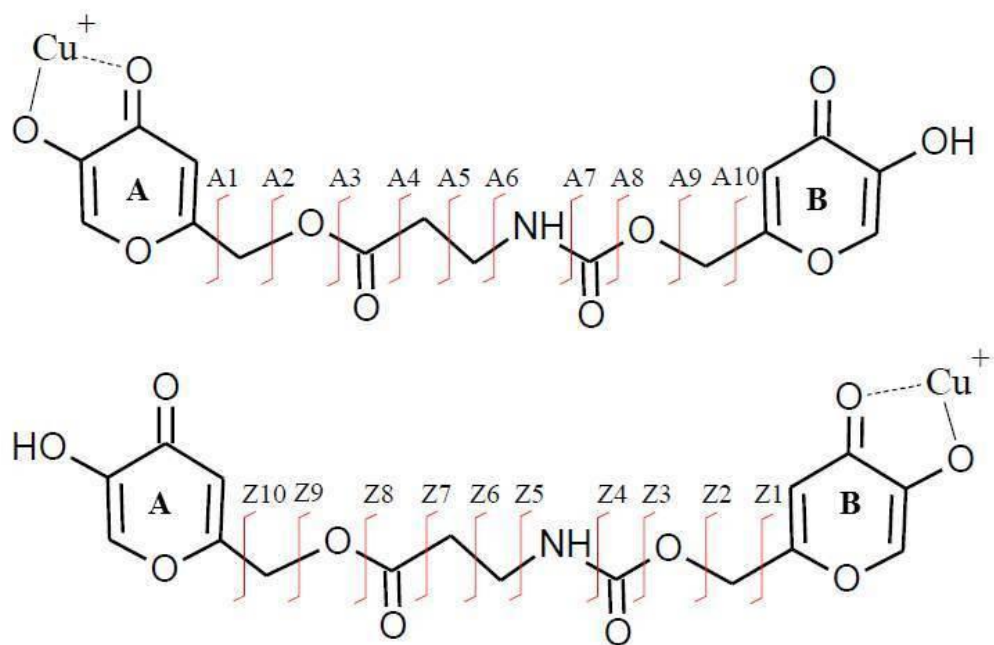


Figure 3

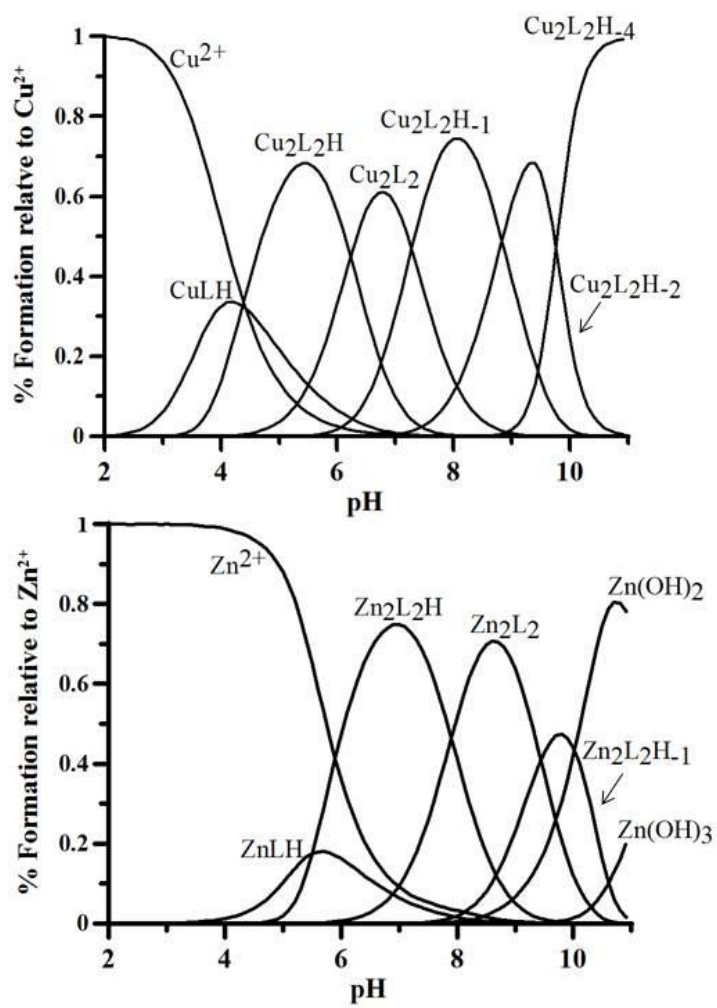


Figure 4

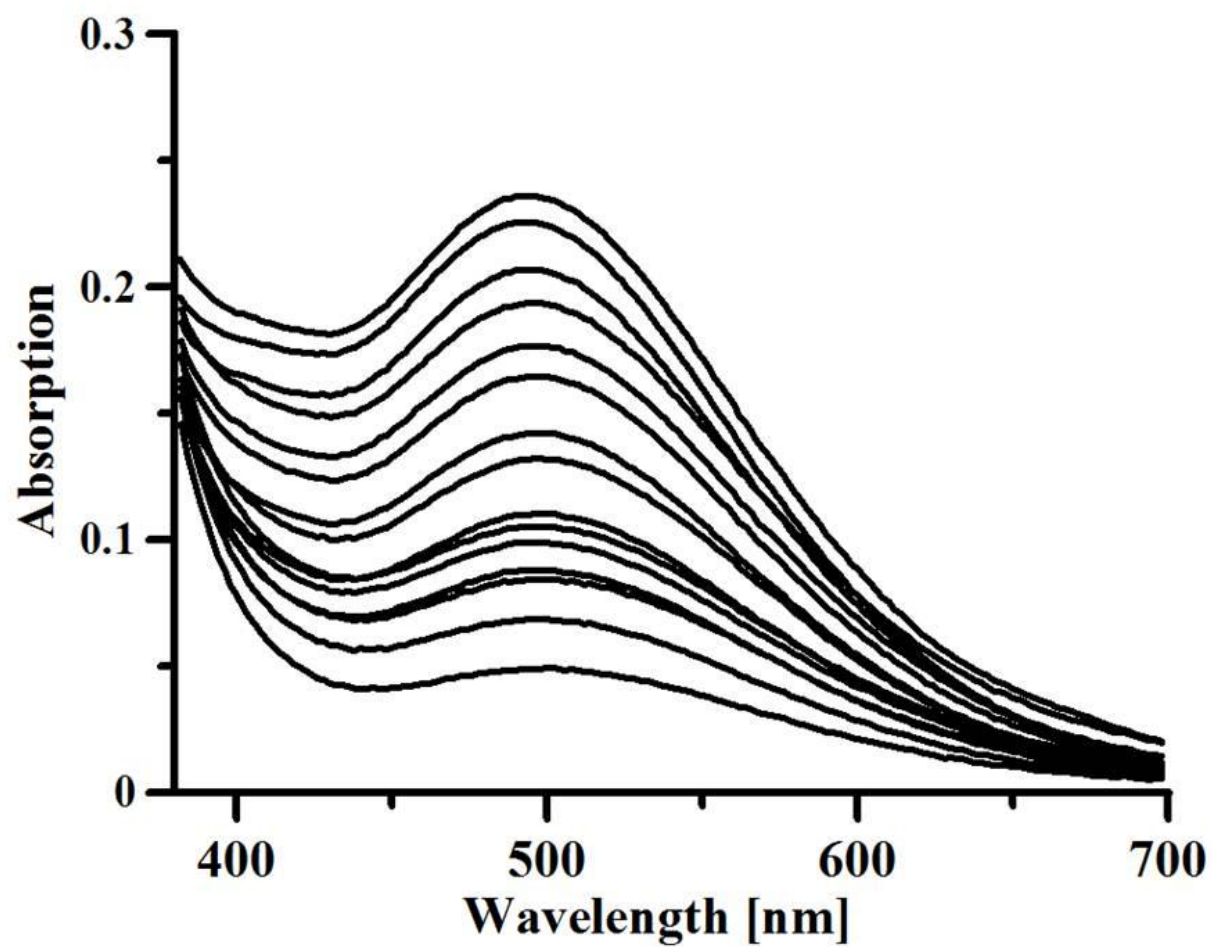


Figure 5

ACCL

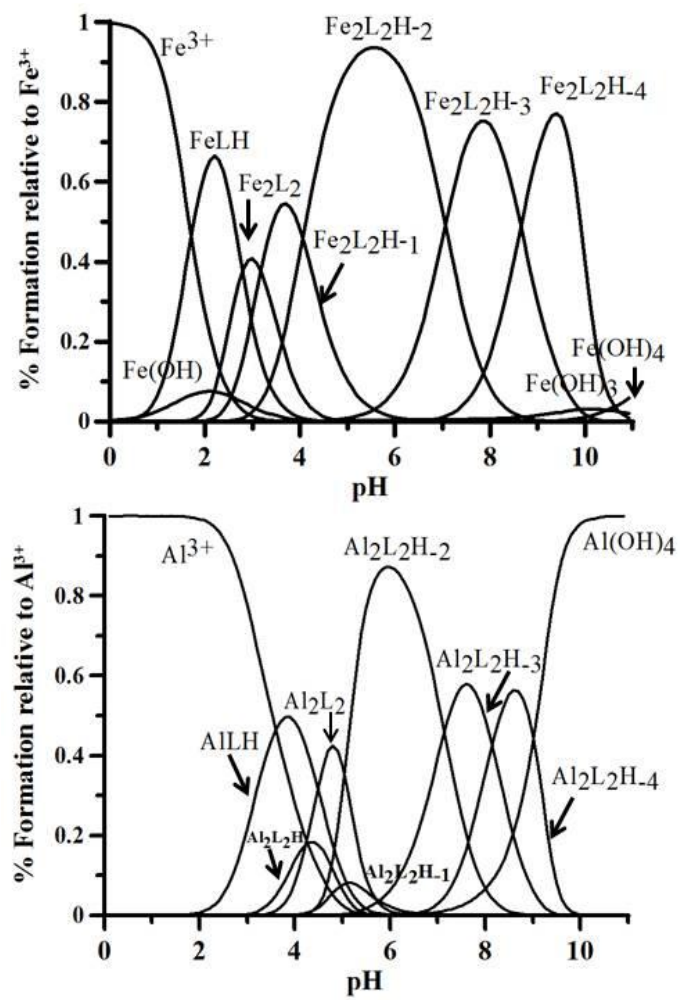


Figure 6

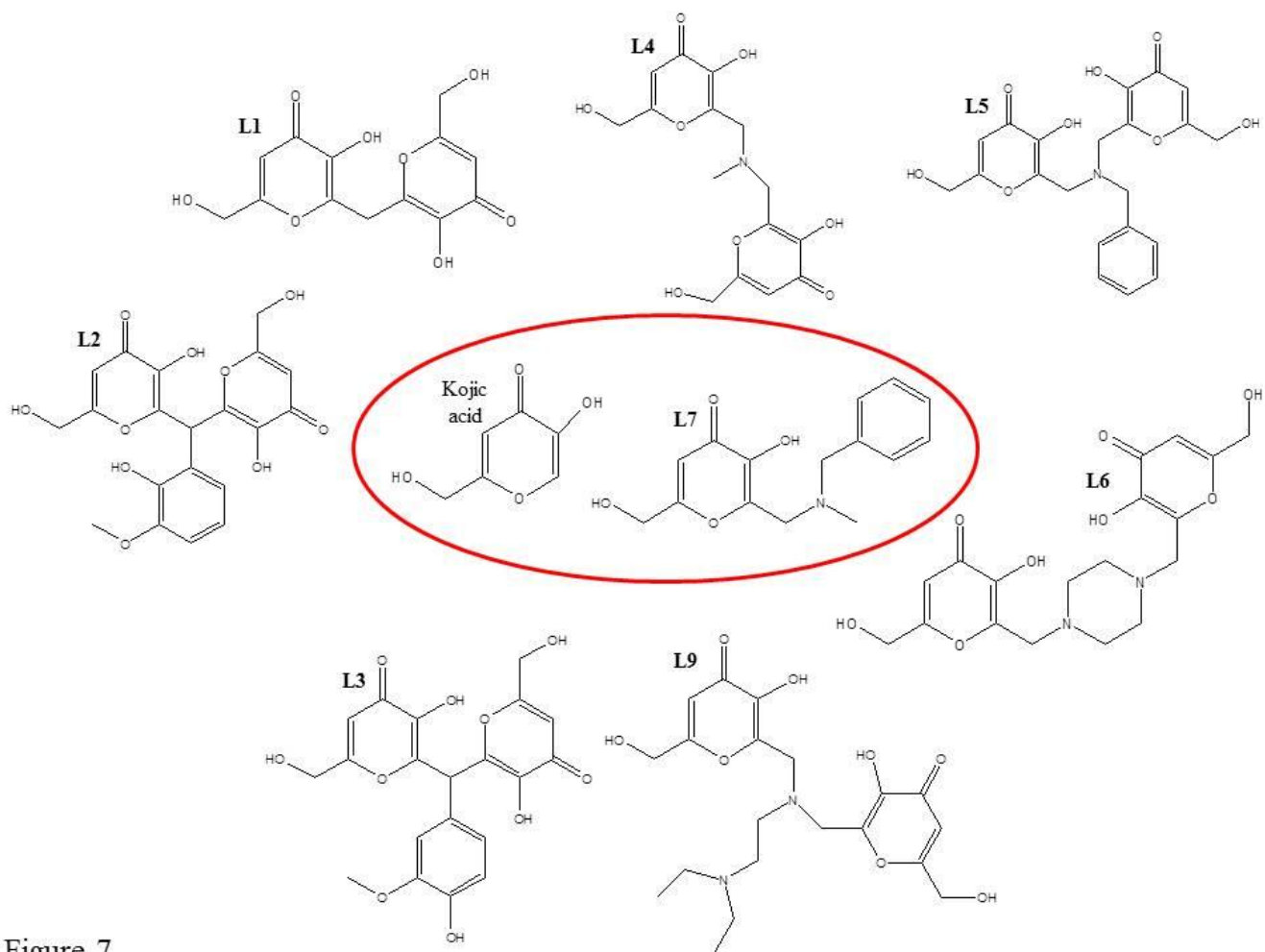


Figure 7

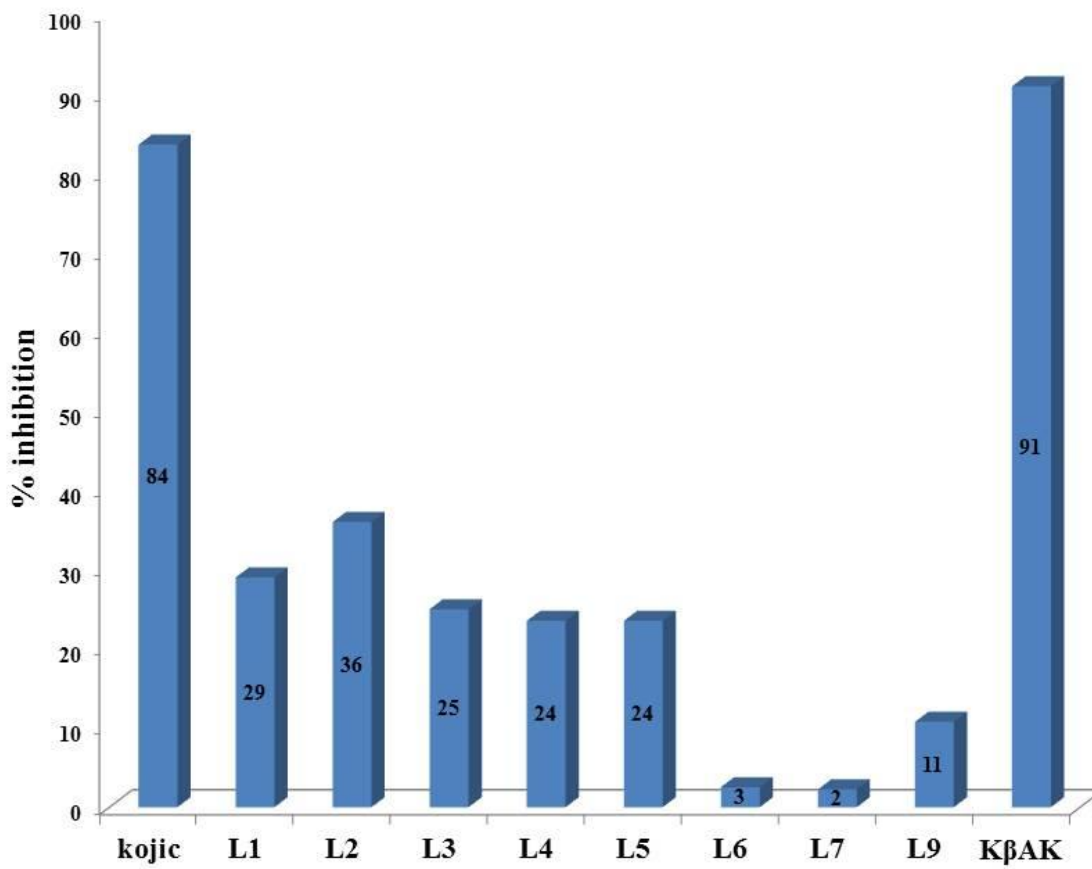


Figure 8

ACCL

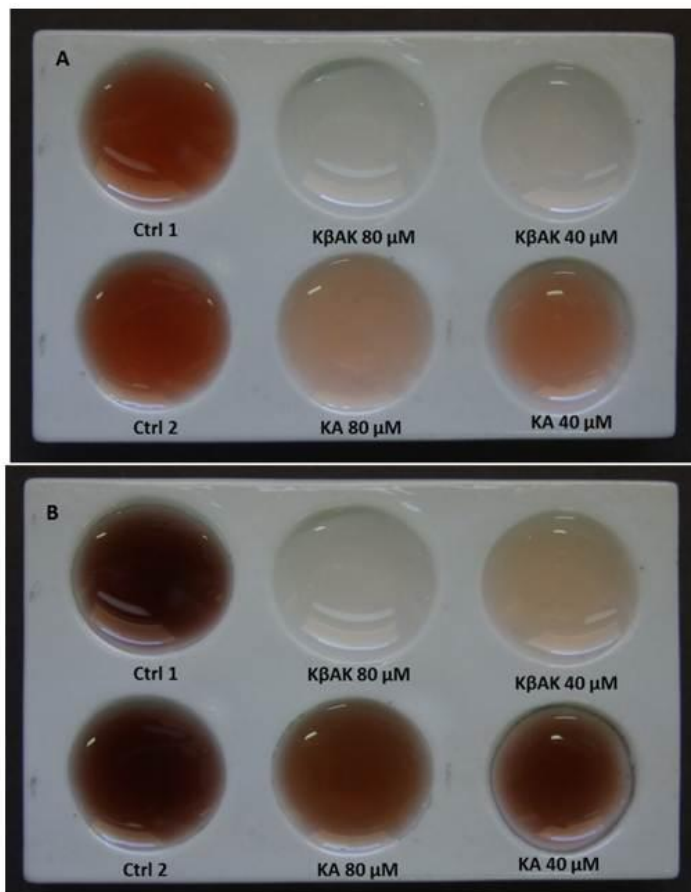
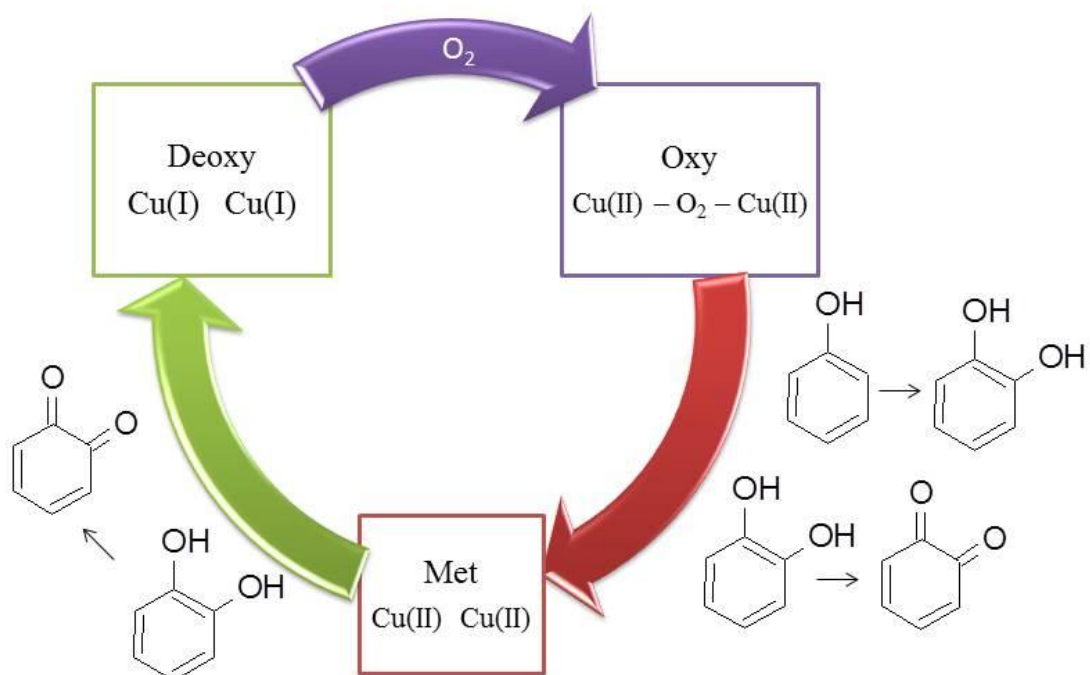


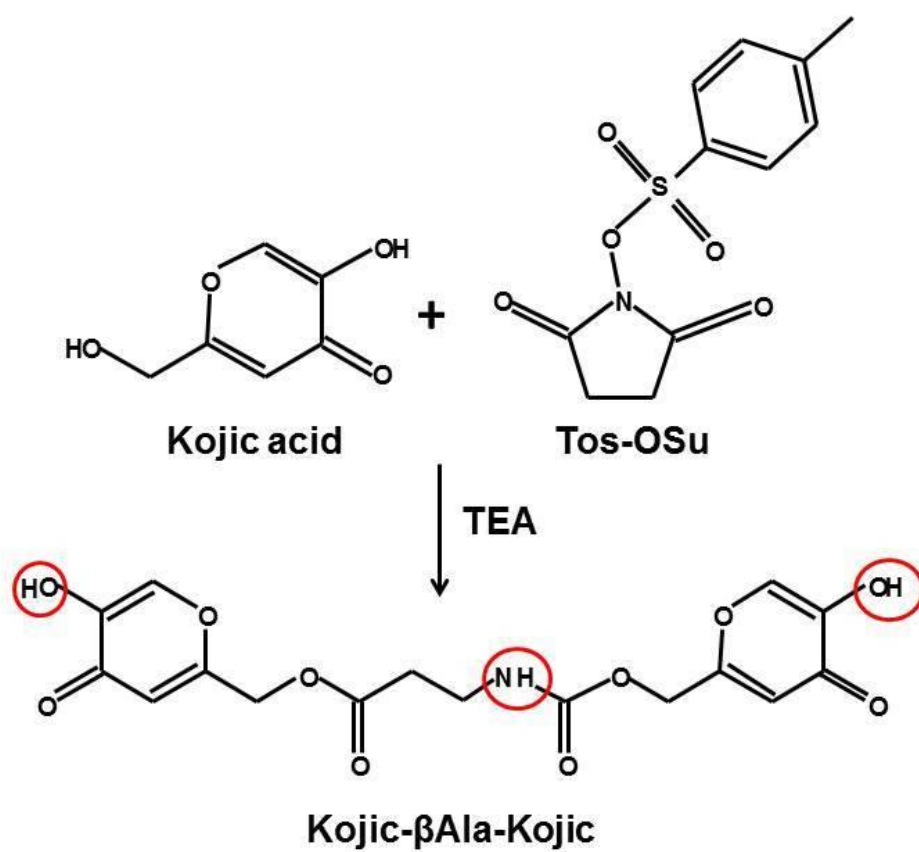
Figure 9

ACCL



Scheme 1

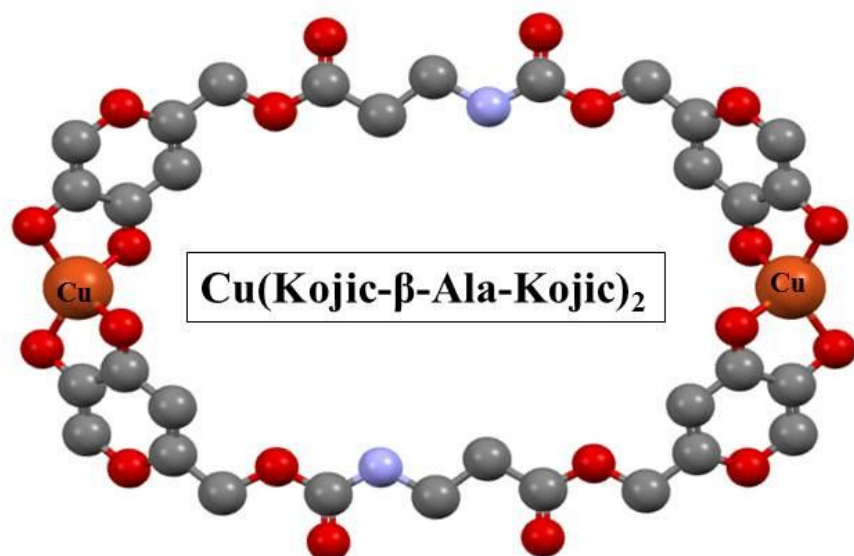
ACCL



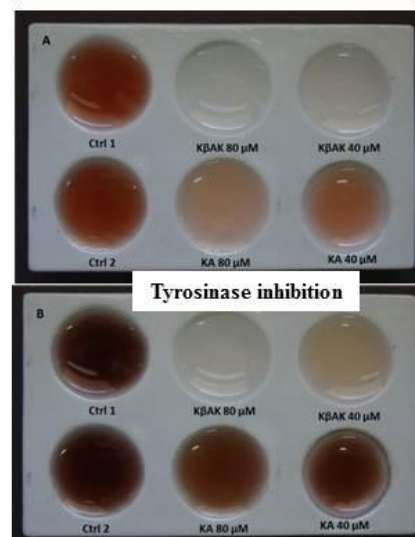
Scheme 2

ACCL

## Graphical Abstract



Tyrosinase inhibition chart



## Pictogram

## Synopsis

Here we describe the synthesis of a new Kojic- $\beta$ Ala-Kojic molecule, metal coordination studies and its tyrosinase inhibitory potential compare to previously synthesized molecules. Kojic- $\beta$ Ala-Kojic exhibited affinity for metal ions and a strong tyrosinase inhibitory effect due to the proper length and kind of linker between two kojic acid units.

**Highlights**

- Synthesis of a new Kojic- $\beta$ -Ala-Kojic acid derivative
- Kojic- $\beta$ -Ala-Kojic is a potent tyrosinase inhibitor
- Stability of  $\text{Cu}^{2+}$ ,  $\text{Zn}^{2+}$ ,  $\text{Fe}^{3+}$ ,  $\text{Al}^{3+}$  complexes
- Possible explanation of the inhibitory activity

ACCEPTED MANUSCRIPT